JOURNAL OF MATERIALS SCIENCE: MATERIALS IN MEDICINE 7 (1996) 623–628

Chemical characterization of *in vivo* aged zinc phosphate dental cements

J. MARGERIT, B. CLUZEL
Faculté d'Odontologie, Montpellier, France
J. M. LELOUP, J. NURIT, B. PAUVERT, A. TEROL
Laboratoire de Chimie Générale et Minérale, Faculté de Pharmacie, Montpellier, France

The chemical composition of zinc phosphate dental cements aged *in vivo* was studied. Twenty-seven samples aged 2 to 43 years were investigated using X-ray diffraction, infrared spectroscopy, ^{31}P nuclear magnetic resonance spectroscopy, thermogravimetric analysis and differential scanning calorimetry. Evidence for the presence of zinc oxide, amorphous zinc phosphate, water of hydration and crystalline zinc phosphate tetrahydrate was found. The latter was identified as hopeite; it was present in 92% of the cements studied. No correlation with time concerning either the chemical structure of the components or their relative amounts was found. Zinc phosphate dental cements show very good chemical stability on long-term use.

1. Introduction

Despite the great popularity of zinc phosphate dental cements, fundamental studies on their chemistry are not numerous. Craig [1], Skinner and Phillips [2], and Servais and Cartz [3] essentially focused on the understanding of the setting reaction. The chemical evolution of zinc phosphate cements with time, although of crucial importance, has only been studied *in vitro* and over a relatively short period (24 h to 6 months) [4, 5]. In an attempt to clarify chemical changes in zinc phosphate dental cements in the oral environment, a study of the ageing of dental phosphate cements *in vivo* was performed. Investigations of the long-term structural and chemical changes of dental cements were performed on powdered samples using X-ray diffraction (XRD), infrared (IR) absorption spectroscopy, ^{31}P magic angle spinning – nuclear magnetic resonance (MAS–NMR) spectroscopy and thermoanalytic techniques: thermogravimetric analysis (TGA) and differential scanning calorimetry (DSC). These techniques were applied to both cements aged in the oral environment for up to 43 years and to freshly prepared cement (48-h-old) for comparison.

2. Materials and methods

In vivo cements: 27 samples of cements were taken after removal of fixed prostheses. All the cement present in these prostheses (inside and outside the crown) was used as samples. None of the occlusals of these prostheses were perforated. A minimum of 30 mg of cement was necessary to perform all the different manipulations. The mean age was 18 years, the oldest being 43 years and the most recent 2 years. Fig. 1 shows the distribution of samples relative to their age. All samples were identified by X-ray diffraction analysis and infrared spectroscopy as zinc phosphate dental cements.

In vitro cement: a typical commercial dental phosphate cement ("Phospha-Cap", from Ivoclar) was prepared for comparison with *in vivo* cements. The powder (ZnO and MgO: 95%) and the liquid (55% H_3PO_4 in water) were mechanically mixed (5 s, 4000 vibrations/min) according to the manufacturer's instructions. All the analyses were performed after at least a 48 h delay (to ensure that the cement was stabilized) [2].

Both *in vivo* and *in vitro* samples were dried in air under ambient conditions (20 °C, 65% RH) and mechanically mixed to obtain fine powders.

X-ray diffraction patterns were obtained with an automatic Phillips diffractometer controlled by an IBM PC (100 acquisitions, 3–35°θ, 1600 points, acquisition delay 500 ms) using anticathode CuK_α (0.15418 nm) with Ni filter.

Infrared absorption spectra were registered on an FT-Bomen DA 8 spectrometer, driven by a VAX 3100 computer, in the 4000–400 cm^{-1} interval. Samples were diluted (1% wt/wt) in vacuum-dried KBr (Aldrich Chemicals, spectroscopic grade), and pellets were made 13 mm diameter, 0.2 mm thickness, under 9 $kN\,cm^{-2}$ pressure.

Solid-state high-resolution ^{31}P nuclear magnetic resonance spectra were obtained using magic angle spinning (^{31}P MAS–NMR). A Brucker AM 300 7 T spectrometer was used, operating at 121.5 MHz and ambient probe temperature. Samples were used as powders. Other experimental conditions were: spinning speed about 5000 Hz, scanning domain 30 kHz, pulses emitted at 90°, pulse width 3 ms, delay between

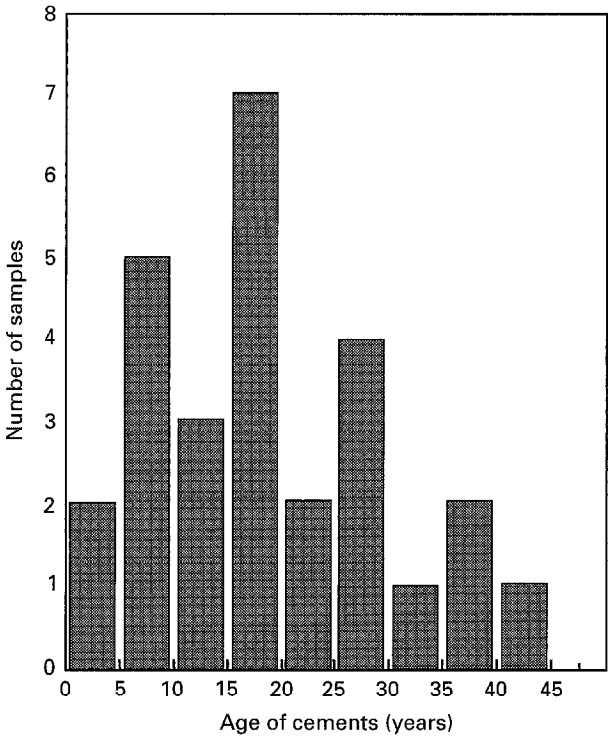

Figure 1 Distribution of the number of cement samples tested versus their age.

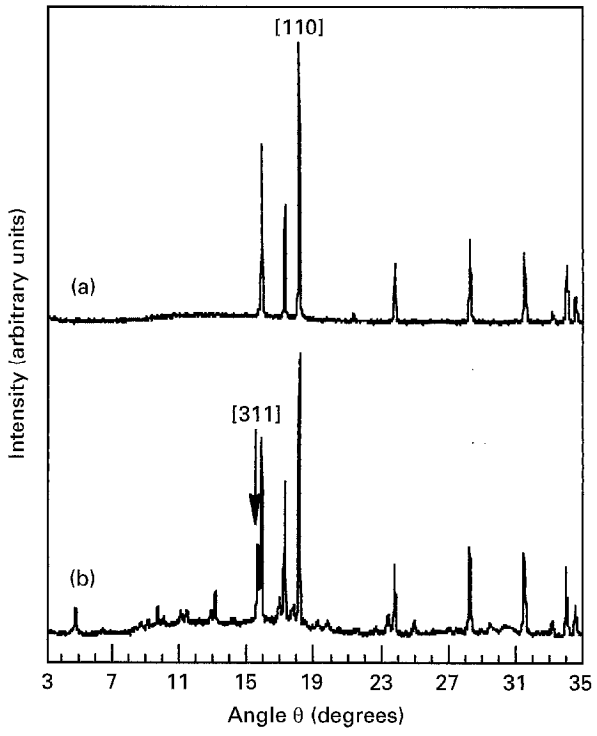

Figure 2 X-ray diffraction patterns of (a) a fresh dental zinc phosphate cement; (b) an *in vivo*, 17-year-old dental cement chosen as an example. The most intense signals for ZnO and hopeite are indicated, and their corresponding Miller plane indices [1 1 0] and [3 1 1], respectively, are given.

pulses 5 s, all spectra were recorded with 100 accumulations. Chemical shifts are reported with respect to the signal of phosphoric acid (H_3PO_4 85%) as external reference.

Thermogravimetric analysis was performed using a Setaram thermobalance with continuous registering, B 601 Ugine-Eyrand systém, and temperature controller RT 64.

Differential scanning calorimetry was realized using a DSC4 Perkin-Elmer computer-managed calorimeter. The calorimetric and thermometric reference was indium. All experiments were executed under nitrogen flow, on 2–3 mg samples in closed pellets. The heating rate was 20 °C min^{-1}.

3. Results

3.1. X-ray diffraction

The X-ray diffractogram (XRD) of the fresh commercial cement is shown in Fig. 2a. Fine diffraction lines corresponding clearly to unreacted crystalline ZnO can be seen. No peak corresponding to MgO is seen. With the sharp peaks of ZnO, a large band coexists in the $8° < \theta < 20°$ domain. Fig. 2b is the XRD diagram of a typical 17-years-old cement aged *in vivo* chosen as an example. All the diffractograms of old cements showed the same crystalline peaks corresponding to ZnO and the same broad band, just as in freshly prepared cement. As few of the samples showed minor peaks due to excess MgO, and nearly all of them showed a series of new peaks.

3.2. Infrared spectroscopy

The infrared spectrum of fresh cement is shown in Fig. 3a, and a typical spectrum of a 12-year-old cement aged *in vivo* is shown for comparison (Fig. 3b). Significant differences may be seen in the 1000 cm^{-1} region. In the spectrum of the fresh cement there is a unique strong broad absorption band centred at 1065 cm^{-1}; whereas in the spectrum of the old cements three sharp bands at about 1020 cm^{-1}, 1080 cm^{-1} and 1120 cm^{-1} are superimposed upon the latter broad band and a single strong sharp band appears at 950 cm^{-1}.

3.3. ^{31}P MAS–NMR spectroscopy

Fig. 4a shows the ^{31}P MAS–NMR spectrum of the fresh cement and Fig. 4b, 4c and 4d show examples of cements aged *in vivo* 7, 17 and 30 years, respectively. All spectra show first-order spinning sidebands in the scanned domain, on either side of the main signals. Apart from the spinning sidebands, the following signals are observed: the fresh cement shows three signals: δ_A, a sharp, intense signal situated at 3.9 ppm; δ_B, a sharp, weak signal situated at 0.2 ppm; and δ_L, a large signal approximately centred at -6.5 ppm. For old cements, the δ_L signal disappears, δ_A remains the most important, δ_B shifts slightly downfield with age; and a new signal $\delta_{A'}$ appears upfield between 3.8 and 4.9 ppm.

3.4. Thermal analysis

For the fresh cement, a 6% weight loss is observed in the TGA curve, beginning at 40 °C and ending at about 100 °C. No other change is observed at higher

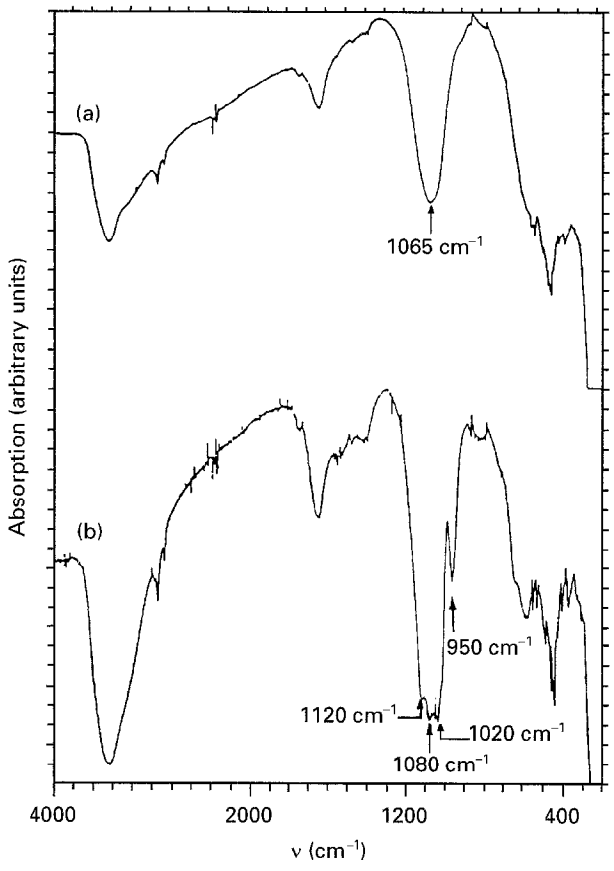

Figure 3 Infrared spectra of (a) a fresh dental zinc phosphate cement; (b) an *in vivo*, 12-year-old dental cement chosen as an example. Bands in the 1000 cm^{-1} regions are indicated.

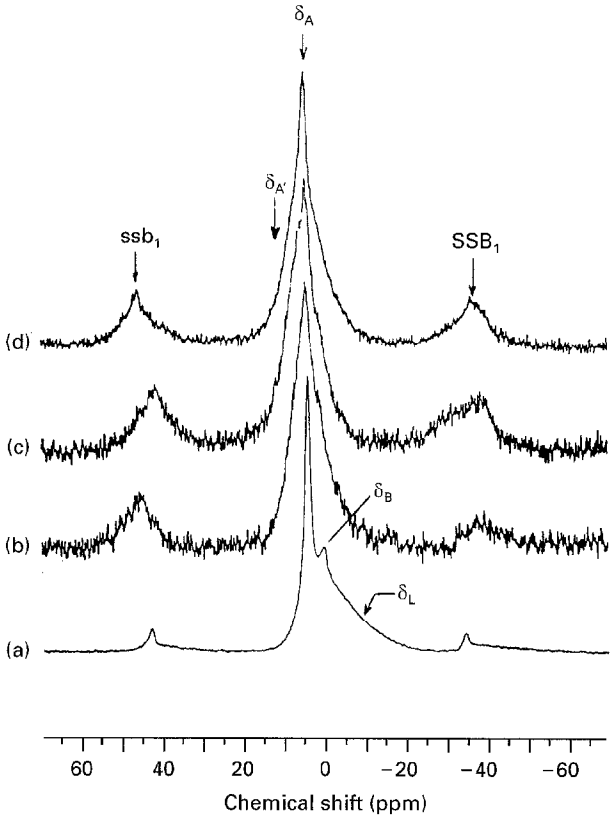

Figure 4 ^{31}P MAS–NMR spectra of (a) a fresh dental zinc phosphate cement; (b) an *in vivo*, 7-year-old dental cement; (c) an *in vivo*, 17-year-old dental cement; and (d) an *in vivo*, 30-year-old dental cement. δ_A, amorphous zinc phosphate; $\delta_{A'}$, crystalline zinc phosphate (hopeite); δ_L, hydrated phosphoric acid or metastable amorphous zinc phosphate; δ_B, unreacted phosphoric acid; SSB_1, highfield spinning sideband; ssb_1, lowfield spinning sideband.

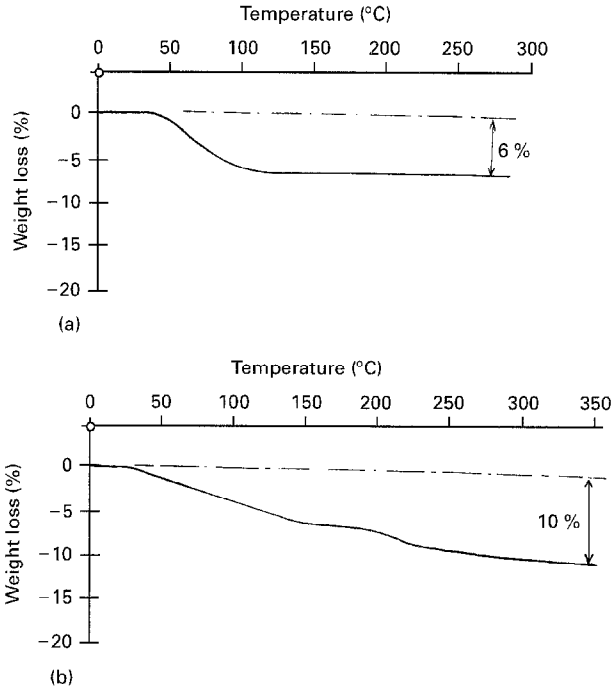

Figure 5 TGA curves for (a) a fresh dental zinc phosphate cement; (b) an *in vivo*, 27-year-old dental cement.

temperatures until the end of the scanned domain is reached at 240 °C (Fig. 5a).

For old cements, the shape of the TGA curve is different, as shown for a 27-year-old cement (Fig. 5b). A first weight loss of 4–8% begins at 40 °C and ends at about 100 °C, as for the fresh cement, but the TGA curve shows a second weight loss (usually 2–4%) starting at about 100–140 °C and finishing about 180–240 °C. The overall weight loss for old cements (10%) is more important than for a fresh cement, and is not dependent on age.

DSC measurements are shown in Fig. 6a and 6b, and correspond to the fresh cement and a 27-year-old cement, respectively. The fresh cement shows an endotherm, $\Delta H_1 = 100\,J\,g^{-1}$, situated at 100 °C. This endotherm remains for old cements, although with smaller values, the average value for the 27 samples being $\Delta H_1 = 17.9\,J\,g^{-1}$. A second endotherm often appears at about 180 °C, but only for samples for which new peaks are revealed by XRD. Its corresponding average energy is $\Delta H_2 = 10.8\,J\,g^{-1}$.

4. Discussion

4.1. X-ray diffraction

The system of diffraction lines observed by XRD for fresh cement corresponds to crystalline ZnO, as is clearly shown by comparison with the ASTM card N°36–1451 (Table I). The diffuse band in the 8–20°θ domain is typical of non-crystalline materials. Since Brady [6] has shown that amorphous phosphates usually show such broad bands in the same diffraction angle range, the diffuse band we observed can be attributed to amorphous zinc phosphate. Therefore, the cement must be a composite of unreacted zinc oxide and amorphous zinc phosphate resulting from the setting reaction of zinc oxide with phosphoric acid and water.

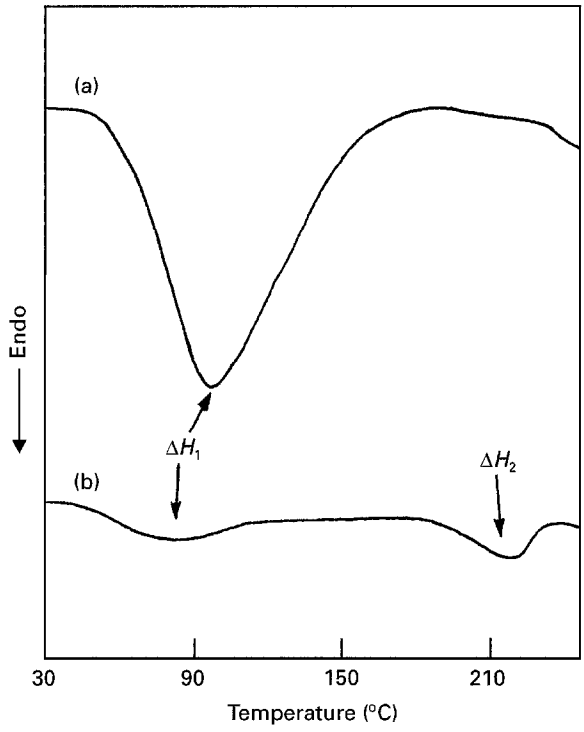

Figure 6 DSC curves for (a) a fresh dental zinc phosphate cement; (b) an *in vivo*, 27-year-old dental cement. Endotherms are labelled ΔH_1 and ΔH_2.

These results are in accordance with the core-link structure proposed for phosphate dental cements [1].

For old cements, a new series of peaks appears. These peaks can be unambiguously attributed (ASTM card N°26–1397) to the crystalline form $Zn_3(PO_4)_2$, $4H_2O$ (an isostructure of the natural mineral "hopeite"). Taking into account the appearance of crystalline zinc phosphate, all the observed peaks can be indexed. Table I gives the indexation of all peaks found for a 17-year-old cement.

Whitaker [7] found that hopeite crystallizes in the orthorhombic system: space group *Pnma*, the cell dimensions are $a = 1.063$ nm, $b = 1.834$ nm, $c = 0.504$ nm. The structure consists of ZnO_6 octahedra, ZnO_4 tetrahedra, and PO_4 tetrahedra, all significantly distorted, and four water molecules. These crystals show poor mechanical properties and can be easily broken.

In *in vitro* XRD, IR, and SEM experiments relative to the setting process, Jakeman *et al.* [8] and Crisp *et al.* [9] found that crystalline zinc phosphate appears at the surface of the cement, and Cartz *et al.* [4] found that its erosion creates a gap between the cement and the dentine substrate. Growing of crystalline hopeite is favoured by high temperature and humidity, whereas aluminium ions or magnesium oxide strongly inhibit its formation. Hopeite does not appear during the setting process itself as shown in Fig. 2a, concerning the fresh cement, but it is clear that the buccal environment favours its development.

Using XRD measurements, it is possible to roughly quantify the amounts of unreacted zinc oxide, amorphous zinc phosphate, and hopeite. The method consists in measuring the intensities of chosen characteristic signals for zinc oxide, hopeite, and amorphous zinc phosphate. These signals are the [1 0 1] ZnO reticular plane, the [3 1 1] hopeite reticular plane and the top of the amorphous zinc phosphate broad band (at 16.5°θ). The values retained for the XRD peak intensities take into account the amorphous contribution, basic line distorsions, number of scans and recording time. No correlation between these signals and the age of the cements was observed, as shown in Fig. 7.

TABLE I Indexation of the XRD lines of a 17-year-old zinc phosphate dental cement[a]

Cement d_{hkl}	ZnO[b] d_{hkl}	[hkl]	Hopeite[c] d_{hkl}	[hkl]
0.909			0.916	020
0.532			0.529	200
0.508			0.508	210
0.485			0.484	011
0.457			0.456	220
0.446			0.441	220
0.400			0.400	230
0.387			0.388	031
0.364			0.365	201
0.345			0.347	240
0.338			0.338	221
0.313			0.313	231
0.285			0.285	311
0.281	0.281	100		
0.264			0.264	400
0.259	0.260	002	0.260	331
0.252			0.251	002
0.247	0.248	101		
0.244			0.242	022
0.233			0.234	261
0.227			0.227	421
0.210			0.210	280
0.200			0.200	460
0.194			0.194	511
0.191	0.191	102		
0.182			0.182	262
0.169			0.169	362
0.163	0.162	110		
0.160			0.160	522
0.156			0.156	641
0.152			0.153	660
0.147	0.148	103		
0.141	0.141	200		
0.138			0.138	112
0.136			0.136	201

[a]Reticular distances d_{hkl} are in nanometres (nm) and the [hkl] are the Miller indices of the corresponding planes
[b]Values from ASTM card N°36-1451
[c]Values from ASTM card N°26-1397

4.2. Infrared spectroscopy

The unique broad absorption band observed at about 1000 cm^{-1} for fresh cement by infrared spectroscopy corresponds to the asymmetric stretching vibration ν_{PO} of the P–O bonds [10]. The presence of a unique band is significant of a highly symmetric environment for the phosphate groups. In that case, the totally symmetric stretching mode is IR-inactive, and the asymmetric stretching mode is triply degenerate. A highly symmetric environment exists naturally in amorphous zinc phosphate, where there is no long-range order, and confirms the formation of amorphous zinc phosphate during the setting process.

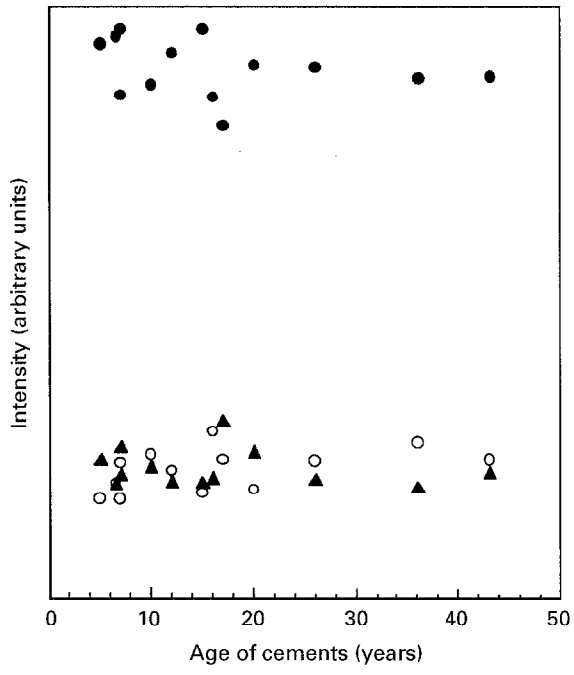

Figure 7 XRD signals intensities versus cement age for (●), residual ZnO; (▲), amorphous zinc phosphate; (○), crystalline zinc phosphate.

The spectrum of the old cement presents several bands in the 1000 cm^{-1} region. Three of them (close to 1000 cm^{-1}) correspond to the asymmetric stretching mode, no longer degenerate, and the one situated at 950 cm^{-1} corresponds to the totally symmetric stretching mode of the phosphate group (now IR active because no longer completely symmetric). These bands show that part of the tetrahedral phosphate groups are no longer symmetric; a feature of phosphate groups which participate in the hopeite structure. These suppositions correlate very well with the X-ray observations, the splitting of the 1000 cm^{-1} broad band being seen only in samples for which XRD patterns possess hopeite peaks.

4.3. ^{31}P MAS–NMR spectroscopy

The chemical shift of phosphorus in phosphate groups depends in the first place on the type of atoms bonded (covalent or coordination bonds) to the group and in the second place, on the protonation of the PO_4^{2-} group [11]. Changes in equilibrium position of protons due to the influence of acidic or basic groups surrounding the tetrahedral phosphate lead to changes in chemical shifts. Sternberg [12] has shown that when proton–donor bonds are formed, the chemical shift moves lowfield by about + 3 ppm, and that, conversely, when hydrogen bonds are weaker, chemical shifts move highfield: proton–acceptor bond formation displaces the chemical shift by − 2 to − 4 ppm.

As a consequence, the δ_B signal can be attributed to unreacted phosphoric acid, the shift lowfield (0 to 0.9 ppm) being probably due to long-range zinc influence. This indicates that residual phosphoric acid is present in the fresh cement in an undissociated form.

The large resonance signal δ_L can be attributed on the one hand to $H_2PO_4^-$ or $H_2PO_4^{2-}$ ions, formed upon contact with water and captive in occlusions. On the other hand, it might correspond to metastable zinc hydrogen phosphate species, transitory in the setting reaction. Their existence, as monozinc or bizinc phosphates has been suggested [1]. Old cements never showed such a signal, as illustrated in Fig. 4b to 4d. If δ_L corresponds to dissociated phosphoric acid, this might mean that these species migrate in the buccal medium or react with residual zinc oxide in some way. If the signal is due to transitory reactive species, this probably means that these metastable species finally react to give zinc phosphate cement.

The last signal to be attributed in the fresh cement spectrum is the most intense one, δ_A, and must be that of the amorphous zinc phosphate matrix.

The $\delta_{A'}$ signal seen on old cement spectra can be attributed to crystalline zinc phosphate, hopeite. Sato [13] found that the chemical shift of pure crystalline hopeite is 4.7 ppm, and Jakeman *et al.* [8, 14] found that several variations can occur in the 3.5–6.0 ppm range for zinc phosphate crystalline systems with a hopeite structure, in which some of the zinc atoms are substituted by divalent metal atoms, such as Mg^{++}, Mn^{++}, Ca^{++}, etc. This signal appears only when XRD patterns show the presence of crystalline phosphate.

4.4. Thermal analysis

Concerning the TGA and DSC analyses it appears that all weight losses observed below 240 °C are due to loss of water because zinc phosphate and zinc oxide evaporate at far higher temperatures. For fresh cement (Fig. 5a), water molecules evaporate below 100 °C and therefore must be weakly bonded to the substrate. Such molecules represent surface water (water of hydration). The absence of subsequent weight loss after 100 °C indicates that no structural water exists in fresh cement, *i.e.* in amorphous zinc phosphate. Most old cements showed weight losses at temperatures up to 240 °C. Weight losses over 100 °C must be attributed to strongly bonded water molecules, that is structural water of crystalline zinc phosphate or hopeite.

Confirmation is given by the DSC analysis. The fresh cements showed one endotherm, which must be that of water of hydration (Fig. 6a). The curves for old cements showed two endotherms (Fig. 6b), one at about 100 °C and another one at about 180 °C. Since the first endotherm corresponds to water of hydration, the second one must be that of structural water of crystalline zinc phosphate. Moreover, Fig. 8 clearly shows that there is a correlation between the presence of the second endotherm (ΔH_2) and the intensity of the [3 1 1] hopeite peak.

Water molecules are captured during crystallization and can come from two sources: external water (buccal) or weakly bonded water (cement surface and occlusions). The strong correlation between ΔH_1 and ΔH_2 (Fig. 9) shows that structural water must originate mainly from water of hydration. There is an increase in the global water content of the cement;

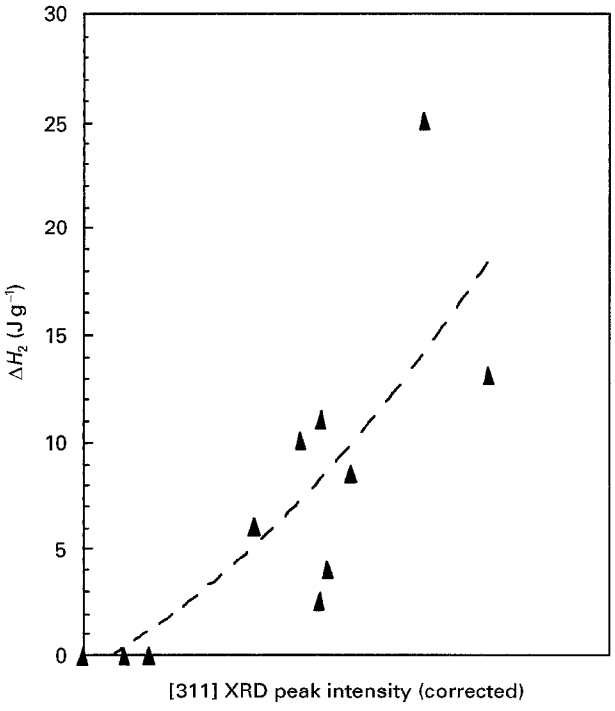

Figure 8 Correlation between the ΔH_2 endotherm and the intensity of the main hopeite peak ([3 1 1] X-ray).

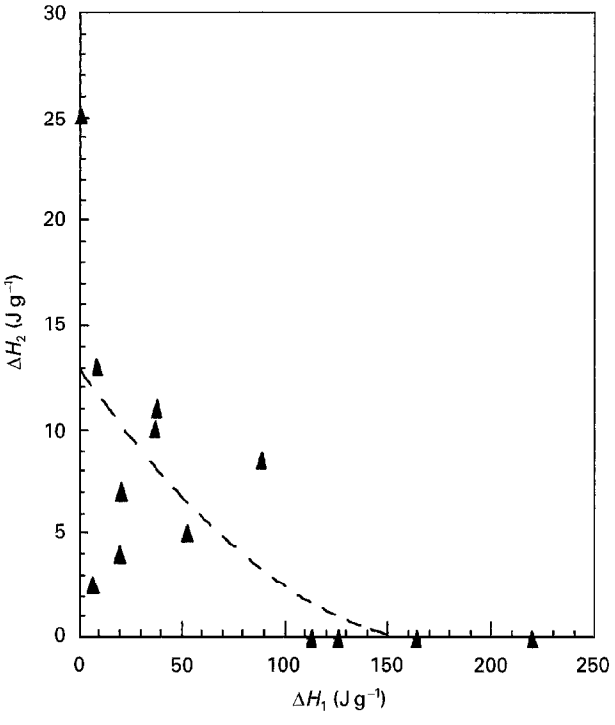

Figure 9 Correlation between the ΔH_2 and the ΔH_1 endotherms.

consequently buccal water must enter the occlusions and microfissures during hopeite crystallization.

5. Conclusion

The present report illustrates the contribution of conventional structural analytical techniques to our understanding of the transformation of zinc phosphate dental cements *in vivo*.

The fresh, 48-h-old, zinc phosphate dental cement investigated contained mainly amorphous zinc phosphate, unreacted zinc oxide and bound water. ^{31}PNMR also showed the presence of unreacted phosphoric acid and probably metastable zinc hydrogen phosphate forms.

Old cements had a different structure. They also contained amorphous zinc phosphate, unreacted zinc oxide and bound water. Neither unreacted phosphoric acid nor metastable zinc hydrogen phosphate is present, and for most of the old cements, a crystalline form identified as hopeite was present. This is the first time that crystals have been observed in *in vivo* aged cements. Their formation corresponds to an increase in the water content of the cement.

These structural changes can occur relatively soon. Once they have taken place, however, the zinc phosphate dental cements were found to be chemically very stable over the time period investigated (from 2 to 43 years). Investigations are currently underway to determine when the transition from the fresh to the stable cements occurs.

References

1. R. G. CRAIG, in "Restorative dental materials" (Mosby, St Louis, 1985) p. 168.
2. E. W. SKINNER and R. W. PHILLIPS, in "Science des matériaux dentaires" (Julien Prélat, Paris, 1971) p. 482.
3. G. E. SERVAIS and L. CARTZ, *J. Dent. Res.* **50** (1971) 613.
4. L. CARTZ, G. SERVAIS and F. ROSSI, *ibid.* **51** (1972) 1668.
5. Y. MATSUYA, M. KODA, Y. YAMAMOTO, S. MATSUYA and M. YAMANE, *Dent. Mater. J.* **2** (1983) 76.
6. G. W. BRADY, *J. Chem. Phys.* **28** (1958) 48.
7. A. WHITAKER, *Acta. Crystallogr.* **B31** (1975) 2026.
8. R. J. B. JAKEMAN, A. K. CHEETHAM, N. J. CLAYDEN and C. M. DOBSON, *J. Solid. State Chem.* **78** (1989) 23.
9. S. CRISP, I. K. O'NEILL, H. J. PROSSER, B. STUART and A. D. WILSON, *J. Dent. Res.* **57** (1978) 245.
10. K. NAKAMOTO, in "Infrared spectra of inorganic and coordination compounds" (Wiley Interscience, New York, 1962) p. 106.
11. J. W. AKITT, in "NMR and chemistry" (Chapman & Hall, London, 1992) p. 17.
12. U. STERNBERG, *Mol. Phys.* **63** (1988) 249.
13. N. SATO, *J. Mater. Sci. Lett.* **10** (1991) 115.
14. R. J. B. JAKEMAN, A. K. CHEETHAM, N. J. CLAYDEN and C. M. DOBSON, *J. Amer. Chem. Soc.* **107** (1985) 6249.

Received 4 April 1995
and accepted 14 March 1996